Intersubband absorption with difference-frequency generation in GaAs asymmetric quantum wells*

Cao Xiao-Long(曹小龙)[a)c)†], Li Zhong-Yang(李忠洋)[b)], Yao Jian-Quan(姚建铨)[a)c)], Wang Yu-Ye(王与烨)[a)c)], Zhu Neng-Nian(朱能念)[a)c)], Zhong Kai(钟 凯)[a)b)], and Xu De-Gang(徐德刚)[a)b)]

[a)] *College of Precision Instrument and Opto-electronics Engineering, Institute of Laser and Opto-electronics, Tianjin University, Tianjin* 300072, *China*

[b)] *Institute of Electric Power, North China University of Water Resources and Electric Power, Zhengzhou* 450011, *China*

[c)] *Key Laboratory of Opto-electronics Information Technology (Tianjin University), Ministry of Education, Tianjin* 300072, *China*

(Received 12 August 2011; revised manuscript received 15 January 2012)

An asymmetric quantum well (AQW) is designed to emit terahertz (THz) waves by using difference frequency generation (DFG) with the structure of GaAs/$Al_{0.2}Ga_{0.8}As$/$Al_{0.5}Ga_{0.5}As$. The characteristics of absorption coefficients are analysed under the parabolic and non-parabolic energy-band conditions in detail. We find that the absorption coefficients vary with the two pump optical intensities, and they reach the maxima when the pump wavelengths are given as $\lambda_{p1} = 9.70$ μm and $\lambda_{p2} = 10.64$ μm, respectively. Compared with non-parabolic conditions, the total absorption coefficient under parabolic conditions shows a blue shift, which is due to the increase in the energy difference between the ground and excited states. By adjusting the two pump optical intensities, the wave vector phase-matching condition inside the AQW is satisfied.

Keywords: asymmetric quantum wells, absorption coefficient, THz-wave, phase-matching

PACS: 42.50.Nn, 78.67.De, 42.65.–k, 61.72.uj **DOI:** 10.1088/1674-1056/21/8/084207

1. Introduction

Efficient terahertz (THz) sources continue to attract world-wide research interest for their potential applications in spectroscopy, biomedical diagnostics, communication, and so on.[1−6] However the potentials of these applications have not been fully realized due to the limited power levels currently available from terahertz sources. Among different schemes for terahertz generation, difference frequency generation (DFG) of the two closely spaced laser frequencies ω_1 and ω_2 in a nonlinear optical crystal is one of the most promising methods to produce high-power, narrow-band coherent, tunable THz-wave in nonlinear crystals.[7−11]

Among nonlinear crystals, GaAs has a large nonlinear coefficient, a wide transparency range, a high damage threshold, and a good thermal conductivity. It is suitable for asymmetric quantum well (AQW) design because its energy and value of the transition can be tailored by changing the geometry of the well in the THz field. In addition, a large $\chi_{(2)}$ in the GaAs quantum well structure can also be achieved by tailoring them so that all interacting fields are in resonance with the intersubband transitions.[12]

However, nonlinear optical crystals have high absorption coefficients in the THz wave region, which restricts the interaction length in crystals and lowers the output THz wave power. To solve this problem, it is vital to investigate the absorption properties for avoiding the maximum absorption and improving the photon utilization rate.

In this paper, the structure of a GaAs AQW is designed for two mixed CO_2 laser beams and the influences of absorption coefficients are discussed. Through adjusting the pump optical intensity, the phase-matching conditions are satisfied.

*Project supported by the National Natural Science Foundation of China (Grant Nos. 60801017, 61172010, 61101058, and 61107086) and the Fund from the Science and Technology Committee of Tianjin, China (Grant No. 11JCYBJC01100).

†Corresponding author. E-mail: caoxiaolong63@126.com

© 2012 Chinese Physical Society and IOP Publishing Ltd

2. Theory

We consider an AQW composed of four different semiconductor layers, which are located at $z < 0$ (layer 1), $0 < z < L_1$ (layer 2), $L_1 < z < L_2$ (layer 3), and $z > L_2$ (layer 4).

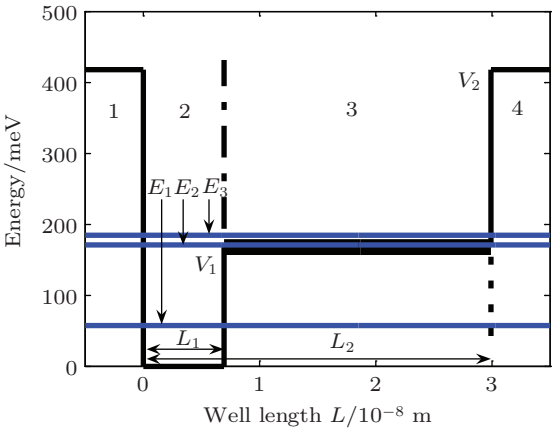


Fig. 1. (colour online) Conduction-band diagram of the structure.

Take a 3-level AQW structure for example, in a nonlinear experiment, two continuous wavelength (CW) and tunable CO_2 lasers P_1 and P_2 can be used to generate two pump waves. The laser P_1, operating at pump wavelength λ_{p1}, is usually tuned in close resonance under the $E_1 \to E_3$ transition, while P_2 is scanned at longer wavelength λ_{p2} and tuned in close resonance with the $E_1 \to E_2$ transition. At the same time, the separation between the E_3 and E_2 subbands is tuned for terahertz emission.

To calculate the linear and nonlinear absorption coefficients, we need to consider the dipole matrix elements and energies of the envelope wave functions. The energy levels E_n and the corresponding envelope wave functions $\varphi_n(z)$ in an AQW can be solved by the Schrödinger equation in the effective mass approach and can be written as follows:

$$\left[-\frac{\hbar^2}{2}\frac{\partial}{\partial z}\left(\frac{1}{m*}\frac{\partial}{\partial z}\right)+V(z)\right]\varphi_n(z)=E_n\varphi_n(z), \quad (1)$$

$$V(z)=\begin{cases}V_2, & z<0,\\ 0, & 0<z<L_1,\\ V_1, & L_1<z<L_2,\\ V_2, & z>L_2,\end{cases} \quad (2)$$

where z represents the growth direction, m^* is the effective mass depending on the material composition.

Under the condition of non-parabolicity, the energy levels can be described by the dispersion relation[13]

$$E=\frac{\hbar^2k^2}{2m*}(1-\gamma k^2), \quad (3)$$

$$\gamma=\frac{\hbar^2}{2m^*}\left(1-\frac{m^*}{m_0}\right)^2\frac{3+4y+2y^2}{3+5y+2y^2}\frac{1}{E_g}, \quad (4)$$

where k is the wave number; γ is the non-parabolicity parameter; $y = \Delta/E_g$ (we take the zero of energy at the bottom of the conduction-band) with Δ being the spin–orbit splitting, and E_g the energy gap; m_0 is the free-electron mass. Generally, we assume that the conduction bands of the well and step layer are non-parabolic and the conduction band of barrier layer is parabolic. So the Schrödinger equation for the wave functions can be obtained after inserting $k \to \mathrm{d}/\mathrm{d}z$ as

$$\hat{H}\psi(z)=-\frac{\hbar^2\gamma(z)}{2m^*(z)}\frac{\mathrm{d}^4}{\mathrm{d}z^4}\psi(z) -\frac{\hbar^2}{2m^*(z)}\frac{\mathrm{d}^2}{\mathrm{d}z^2}\psi(z)+V(z)\psi(z)=E\psi(z). \quad (5)$$

The absorption coefficient $\alpha(\omega)$ can be expressed as

$$\alpha(\omega)=\omega\sqrt{\frac{\mu}{\varepsilon_R}}\,\mathrm{Im}\{\varepsilon_0\chi(\omega)\}, \quad (6)$$

where μ is the permeability of the system, ε_R is the real part of the permittivity, ω is the angular frequency of the incident photon energy, and χ is the nonlinear susceptibility.[14,15] By using the compact density matrix approach and interactive method, the linear and nonlinear changes in the absorption coefficient are given as follows. For the linear term,

$$\alpha^{(1)}(\omega_1)=\omega_1\sqrt{\frac{\mu}{\varepsilon_R}}\frac{N\rho_{11}^{(0)}Z_{13}^2\hbar\Gamma_{31}}{[(E_3-E_1-\hbar\omega_1)^2+(\hbar\Gamma_{31})^2]}, \quad (7)$$

$$\alpha^{(1)}(\omega_2)=\omega_2\sqrt{\frac{\mu}{\varepsilon_R}}\frac{N\rho_{11}^{(0)}Z_{12}^2\hbar\Gamma_{21}}{[(E_2-E_1-\hbar\omega_2)^2+(\hbar\Gamma_{21})^2]}, \quad (8)$$

$$\alpha^{(1)}(\omega_{THz})=\omega_{THz}\sqrt{\frac{\mu}{\varepsilon_R}}\frac{N\rho_{11}^{(0)}Z_{23}^2\hbar\Gamma_{23}}{[(E_3-E_2-\hbar\omega_{THz})^2+(\hbar\Gamma_{23})^2]}; \quad (9)$$

for the third-order term,

$$
\begin{aligned}
&\alpha^{(3)}(\omega_1, I_1, I_2)\\
&= \omega_1\sqrt{\frac{\mu}{\varepsilon_{\rm R}}}\frac{NZ_{13}(\hbar\omega_1-(E_3-E_1))}{[\hbar\omega_1-(E_3-E_1)]^2+(\hbar\Gamma_{31})^2}\Bigg\{-\frac{-\rho_{11}^{(0)}Z_{31}Z_{21}Z_{12}I_2}{[\hbar(\omega_1-\omega_2)-(E_3-E_2)]^2+(\hbar\Gamma_{32})^2}\\
&\times\Bigg\{\frac{\hbar\Gamma_{32}[(E_2-E_1)-\hbar\omega_2]+\hbar\Gamma_{12}[\hbar(\omega_1-\omega_2)-(E_3-E_2)]}{[(E_2-E_1)-\hbar\omega_2]^2+(\hbar\Gamma_{12})^2}\\
&+\frac{\hbar\Gamma_{32}[\hbar\omega_1-(E_3-E_1)]+\hbar\Gamma_{31}[\hbar(\omega_1-\omega_2)-(E_3-E_2)]}{[\hbar\omega_1-(E_3-E_1)]^2+(\hbar\Gamma_{31})^2}\Bigg\}\Bigg\}-\omega_1\sqrt{\frac{\mu}{\varepsilon_{\rm R}}}\frac{NZ_{13}\hbar\Gamma_{31}}{[\hbar\omega_1-(E_3-E_1)]^2+(\hbar\Gamma_{31})^2}\\
&\times\Bigg\{\frac{-\rho_{11}^{(0)}Z_{31}Z_{31}Z_{13}I_1(-\hbar\Gamma_{31})}{[\hbar\omega_1-(E_3-E_1)]^2+(\hbar\Gamma_{31})^2}\frac{4}{\hbar\Gamma_{11}}+\frac{-\rho_{11}^{(0)}Z_{31}Z_{21}Z_{12}I_2}{\hbar\Gamma_{11}}\frac{-2\hbar\Gamma_{21}}{[\hbar\omega_2-(E_2-E_1)]^2+(\hbar\Gamma_{21})^2}\\
&+\frac{-\rho_{11}^{(0)}Z_{31}Z_{21}Z_{12}I_2}{[\hbar(\omega_1-\omega_2)-(E_3-E_2)]^2+(\hbar\Gamma_{32})^2}\Bigg\{\frac{[\hbar(\omega_1-\omega_2)-(E_3-E_2)][(E_2-E_1)-\hbar\omega_2]-\hbar\Gamma_{32}\hbar\Gamma_{12}}{[(E_2-E_1)-\hbar\omega_2]^2+(\hbar\Gamma_{12})^2}\\
&+\frac{[\hbar(\omega_1-\omega_2)-(E_3-E_2)][\hbar\omega_1-(E_3-E_1)]-\hbar\Gamma_{32}\hbar\Gamma_{31}}{[\hbar\omega_1-(E_3-E_1)]^2+(\hbar\Gamma_{31})^2}\Bigg\}\Bigg\},
\end{aligned}
\tag{10}
$$

$$
\begin{aligned}
&\alpha^{(3)}(\omega_2, I_1, I_2)\\
&= \omega_2\sqrt{\frac{\mu}{\varepsilon_{\rm R}}}\frac{NZ_{12}(\hbar\omega_2-(E_2-E_1))}{[\hbar\omega_2-(E_2-E_1)]^2+(\hbar\Gamma_{21})^2}\Bigg\{-\frac{-\rho_{11}^{(0)}Z_{21}Z_{31}Z_{13}I_1}{[\hbar(\omega_1-\omega_2)-(E_3-E_2)]^2+(\hbar\Gamma_{23})^2}\\
&\times\Bigg\{\frac{\hbar\Gamma_{23}[\hbar\omega_2-(E_2-E_1)]+\hbar\Gamma_{21}[(E_3-E_2)-\hbar(\omega_1-\omega_2)]}{[(E_2-E_1)-\hbar\omega_2]^2+(\hbar\Gamma_{21})^2}\\
&+\frac{\hbar\Gamma_{23}[(E_3-E_1)-\hbar\omega_1]+\hbar\Gamma_{13}[(E_3-E_2)-\hbar(\omega_1-\omega_2)]}{[(E_3-E_1)-\hbar\omega_1]^2+(\hbar\Gamma_{13})^2}\Bigg\}\Bigg\}-\omega_2\sqrt{\frac{\mu}{\varepsilon_{\rm R}}}\frac{NZ_{12}\hbar\Gamma_{21}}{[\hbar\omega_2-(E_2-E_1)]^2+(\hbar\Gamma_{21})^2}\\
&\times\Bigg\{\frac{-\rho_{11}^{(0)}Z_{21}Z_{21}Z_{12}I_2(-\hbar\Gamma_{21})}{[\hbar\omega_2-(E_2-E_1)]^2+(\hbar\Gamma_{21})^2}\frac{4}{\hbar\Gamma_{11}}+\frac{-\rho_{11}^{(0)}Z_{21}Z_{31}Z_{13}I_1}{\hbar\Gamma_{11}}\frac{-2\hbar\Gamma_{31}}{[\hbar\omega_1-(E_3-E_1)]^2+(\hbar\Gamma_{31})^2}\\
&+\frac{-\rho_{11}^{(0)}Z_{21}Z_{31}Z_{13}I_1}{[\hbar(\omega_1-\omega_2)-(E_3-E_2)]^2+(\hbar\Gamma_{23})^2}\Bigg\{\frac{[\hbar(\omega_1-\omega_2)-(E_3-E_2)][(E_2-E_1)-\hbar\omega_2]-\hbar\Gamma_{23}\hbar\Gamma_{21}}{[(E_2-E_1)-\hbar\omega_2]^2+(\hbar\Gamma_{21})^2}\\
&+\frac{[\hbar(\omega_1-\omega_2)-(E_3-E_2)][\hbar\omega_1-(E_3-E_1)]-\hbar\Gamma_{23}\hbar\Gamma_{13}}{[\hbar\omega_1-(E_3-E_1)]^2+(\hbar\Gamma_{13})^2}\Bigg\}\Bigg\}.
\end{aligned}
\tag{11}
$$

Then the total absorption coefficient is

$$\alpha(\omega, I_1, I_2) = \alpha^{(1)}(\omega) + \alpha^{(3)}(\omega, I_1, I_2), \tag{12}$$

and thus

$$\alpha_{\omega 1}(I_1, I_2) = \alpha_{\omega 1}^{(1)} + \alpha_{\omega 1}^{(3)}(I_1, I_2), \tag{13a}$$

$$\alpha_{\omega 2}(I_1, I_2) = \alpha_{\omega 2}^{(1)} + \alpha_{\omega 2}^{(3)}(I_1, I_2). \tag{13b}$$

3. Results and discussion

As an example, a 7-nm deep well width, 30-nm shallow well width, $GaAs/Al_{0.2}Ga_{0.8}As/Al_{0.5}Ga_{0.5}$ AQW doped at 1×10^{17} cm^{-3} is considered. In optical device applications, a large induced absorption coefficient changing with pump beam could be used to modulate confinement in optical devices. Such modulation effects are of special interest in the 9 μm–11 μm region, where the refractive index change corresponds to the CO_2 laser lines. So, the following discussion is restricted within this region.

When a semiconductor is fabricated into a very thin layer (e.g., $\sim$ 10 nm), the optical absorption spectrum changes radically as a result of the quantum confinement of carriers in the resulting one-dimensional potential well. Figure 2 illustrates the variations of absorption coefficient $\alpha_{\omega 1}$ as a function of the pump wave $\lambda_{\rm p1}$ at different values of incident intensity I_1 (I_2 = 0.1 MW/cm^2). It is clearly seen that for $I_1 < 0.3$ MW/cm^2, the absorption coefficient $\alpha_{\omega 1}$ increases with the increase of pump wavelength until the maximum value, and then drops down rapidly. When $I_1 > 0.3$ MW/cm^2, there is the bleaching effect at the line centre.

The total absorption coefficient $\alpha(\omega, I_1, I_2)$ consists of two components of $\alpha^{(1)}(\omega)$ and $\alpha^{(3)}(\omega, I_1, I_2)$, so we think that the large positive absorption is due to the $\alpha_{\omega 1}^{(1)}$ contribution and this large absorption is significantly reduced by the $\alpha_{\omega 1}^{(3)}$ contribution. Since the incident optical field contributes only to the $\alpha_{\omega 1}^{(3)}$ term, at sufficiently high intensity the absorption at line centre can be bleached (at I_1 = 0.3 MW/cm^2).

This is illustrated by the series of $\alpha^{(3)}(\omega, I_1, I_2)$ absorption curves at different values of pump intensity I_1. The bleaching effect at the line centre is hinted at only at 0.3 MW/cm^2, and can be quite clear in the 0.6 MW/cm^2. When I_1 reaches 1.0 MW/cm^2, the effect of $\alpha^{(1)}(\omega)$ almost disappears, the characteristics of absorption only show the effect of $\alpha^{(3)}(\omega, I_1, I_2)$, which is related to optical intensity.

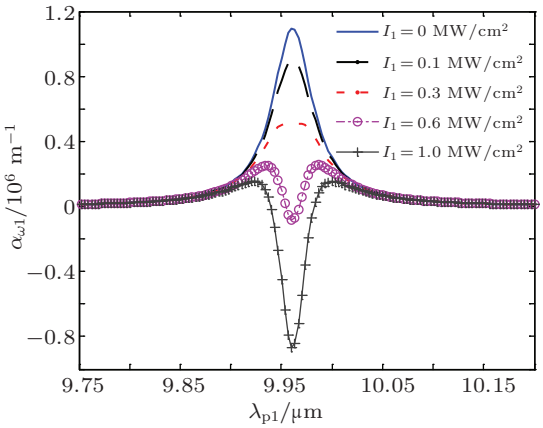


Fig. 2. (colour online) Curves for absorption coefficient $\alpha_{\omega1}$ as a function of pump wavelength λ_{p1} at different values of pump intensity I_1 (I_2 = 0.1 MW/cm^2, λ_{p2} = 10.64 μm).

Figures 2–5 indicate the similar change trends that with the increase of its own pump wavelength, the absorption coefficient increases until a maximal value, then drops down rapidly. However, with the increase of the other pump wavelength, the absorption coefficient has a minimal value. Therefore, we can say that the contributions of both the linear and the nonlinear absorption coefficients should be considered in the calculation of absorption spectrum of the system operating especially with a high pump intensity.

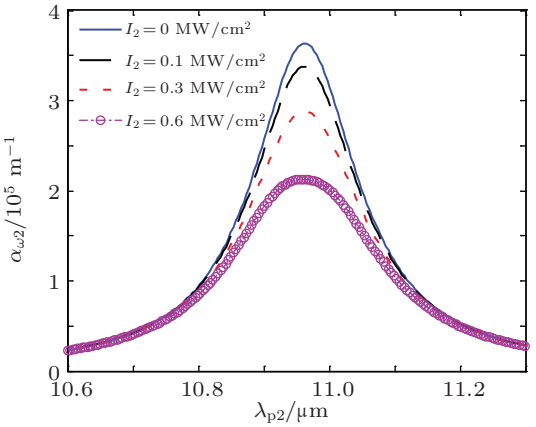


Fig. 3. (colour online) Curves for absorption coefficient $\alpha_{\omega2}$ as a function of the pump wavelength λ_{p2} at different values of pump intensity I_2 (I_1 = 0.1 MW/cm^2 and λ_{p1} = 9.70 μm).

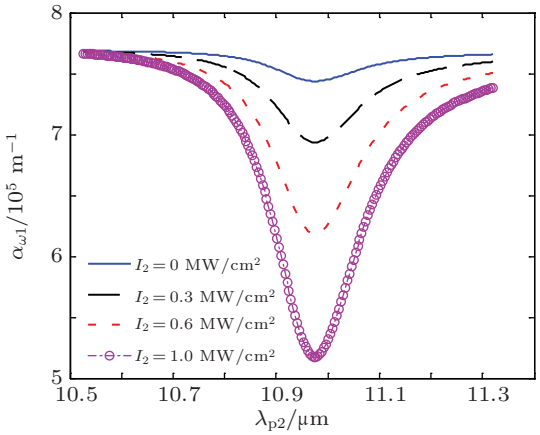


Fig. 4. (colour online) Curves for absorption coefficient $\alpha_{\omega1}$ as a function of the pump wavelength λ_{p2} at different values of pump intensity I_2 (I_1 = 0.1 MW/cm^2 and λ_{p1} = 9.70 μm).

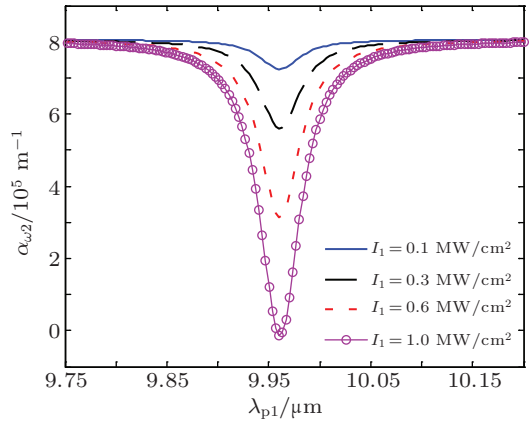


Fig. 5. (colour online) Curves for absorption coefficient $\alpha_{\omega2}$ as a function of the pump wavelength λ_{p1} at different values of pump intensity I_1 (I_2 = 0.1 MW/cm^2 and λ_{p2} = 10.64 μm).

Through solving the Schrödinger equation, we can figure out the energy levels, which are given respectively as E_1 = 58.8381 meV, E_2 = 172.1491 meV, E_3 = 186.1842 meV under the condition of parabolicity, and E_1 = 56.7078 meV, E_2 = 170.0292 meV, E_3 = 181.4327 meV under the condition of non-parabolicity.

From Fig. 6, compared with non-parabolic well, the parabolic well shows a blue shift of absorption coefficient $\alpha_{\omega1}$. This shift can be due to the increase in the energy difference $E_3 - E_1$ between the ground and second excited states. $\Delta E_{31} = (E_3 - E_1)_{\text{parabolicity}} - (E_3 - E_1)_{\text{nonparabolicity}}$ = 2.6212 meV. However, the absorption coefficient $\alpha_{\omega2}$ as seen in Fig. 7, is related to the energy difference $E_2 - E_1$ between the ground and first excited states, the peak value almost remains constant, the $\Delta E_{21} = (E_2 - E_1)_{\text{parabolicity}} - (E_2 - E_1)_{\text{nonparabolicity}} = -0.0104$ meV.

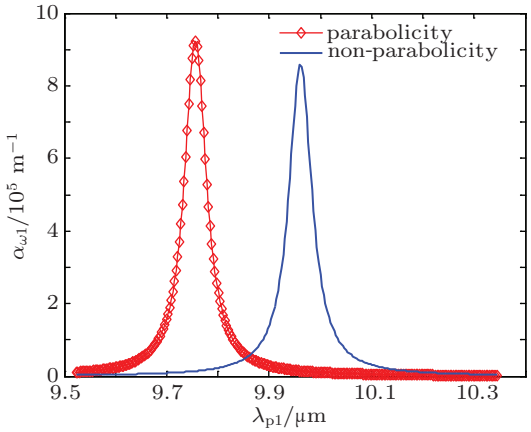


Fig. 6. (colour online) Comparison of absorption coefficient $\alpha_{\omega 1}$ between under parabolic condition and under non-parabolic condition, at pump intensity $I_1 = I_2 = 0.1$ MW/cm^2, $\lambda_{p1} = 9.70$ μm, and $\lambda_{p2} = 10.64$ μm

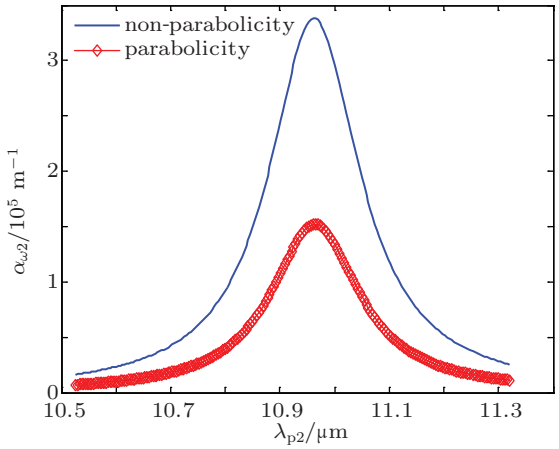


Fig. 7. (colour online) Comparison of absorption coefficient $\alpha_{\omega 2}$ between under parabolic condition and under non-parabolic condition, at pump intensity $I_1 = I_2 = 0.1$ MW/cm^2, $\lambda_{p1} = 9.70$ μm, and $\lambda_{p2} = 10.64$ μm.

Consider the $Al_{0.2}Ga_{0.8}As/GaAs/Al_{0.5}Ga_{0.5}As$ AQW with an optical intensity of 0.1 MW/cm^2, the change of the absorption coefficient α_{THz} as a function of pump wavelength is illustrated in Fig. 8. We can see that the α_{THz} is related to the two pump wavelengths, first decreases and then increases. The maximum is 1.553×10^7 m^{-1} when the two pump wavelengths are 9.70 μm and 10.64 μm, respectively. Therefore, the appropriate α_{THz} in the AQW can be selected by tuning the two pump wavelengths to improve conversion efficiency.

Considering the available wavelength range of CO_2 laser, two pump intensities continuously tunable from 0 to 6 MW/cm^2 are used for calculating the phase mismatch. Figures 9 and 10 show the relations between absorption coefficient and pump intensity. Because the nonlinear section $\alpha^{(3)}$ in absorption coefficient depends on pump intensity, we can select the absorption coefficient through changing the two pump intensities. Figure 11 illustrates the phase mismatch Δk as a function of pump intensities I_1 and I_2 at the pump wavelengths $\lambda_{p1} = 9.70$ μm and $\lambda_{p2} = 10.64$ μm for the structure of AQW well in Fig. 1. In Fig. 9, the intersection of the surface of phase mismatch Δk with

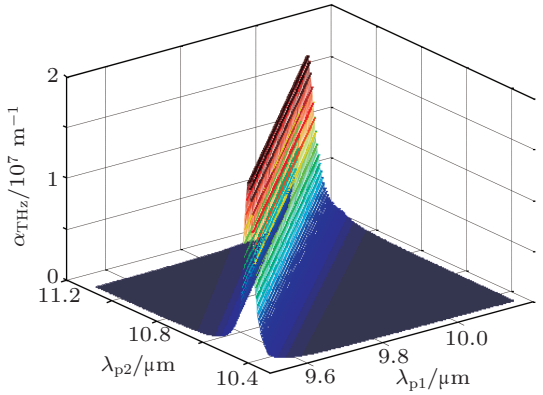


Fig. 8. (colour online) Absorption coefficient α_{THz} as a function of pump wavelength at pump intensity $I_1 = I_2 = 0.1$ MW/cm^2.

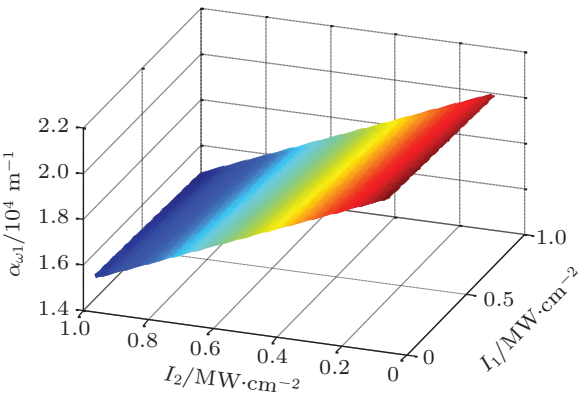


Fig. 9. (colour online) Absorption coefficient $\alpha_{\omega 1}$ as a function of the pump intensities I_1 and I_2 (the pump wavelengths $\lambda_{p1} = 9.70$ μm and $\lambda_{p2} = 10.64$ μm).

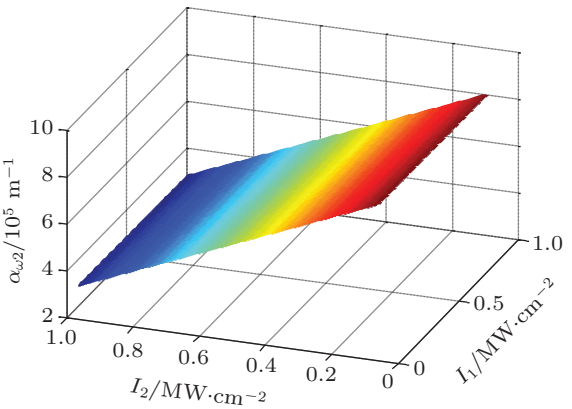


Fig. 10. (colour online) Absorption coefficient $\alpha_{\omega 2}$ as a function of the pump intensities I_1 and I_2 (the pump wavelengths $\lambda_{p1} = 9.70$ μm and $\lambda_{p2} = 10.64$ μm).

the plane of $\Delta k = 0$ satisfies the phase-matching condition. Thus, we can adjust the pump intensity to acquire the phase-matching condition.

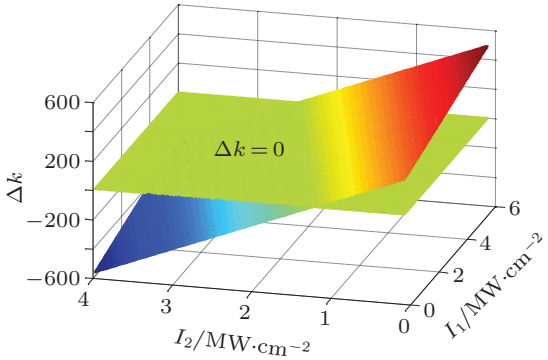


Fig. 11. (colour online) Phase mismatch Δk as a function of the two pump intensities (the pump wavelengths $\lambda_{p1} = 9.70$ μm and $\lambda_{p2} = 10.64$ μm).

4. Conclusion

In this paper, we designed a GaAs/$Al_{0.2}Ga_{0.8}As$/$Al_{0.5}Ga_{0.5}As$ asymmetric quantum well and calculated its absorption coefficient. When the two pump wavelengths are given as $\lambda_{p1} = 9.70$ μm and $\lambda_{p2} = 10.64$ μm, respectively, the peak value of the absorption coefficient reaches 1.553×10^7 m^{-1}. We can obtain an appropriate α_{THz} by adjusting the two pump wavelengths. The phase-matching condition can also be satisfied to generate a THz wave by adjusting the two pump intensities. This study may have profound consequences for practical devices such as THz emission and THz optical switches.

References

[1] Johnson M B, Whittaker D M, Corchia A, Davies A G and Linfield E H 2002 *Phys. Rev.* B **65** 165301
[2] Schmuttenmaer C A 2004 *Chem. Rev.* **104** 1759b
[3] Xie X, Dai J and Zhang X C 2006 *Phys. Rev. Lett.* **96** 075505
[4] Qi C C and Cheng Z H 2009 *Chin. Phys. Lett.* **26** 064201
[5] Bahk Y M, Park H R, Ahn K J, Kim H S, Ahn Y H, Kim D S, Bravo-Abad J, Martin-Moreno L and Garcia-Vidal F J 2011 *Phys. Rev. Lett.* **106** 013902
[6] Li J S and Li X J 2009 *Acta Phys. Sin.* **58** 5805 (in Chinese)
[7] Apollonov V V, Shakir Y A and Gribenyukov A I 2002 *J. Phys.* D: *Appl. Phys.* **35** 1477
[8] Molter D, Theuer M and Beigang R 2009 *Opt. Express* **17** 6623
[9] Staus C M, Kuech T F and Caughan L M 2010 *Opt. Express* **18** 2332
[10] Geng Y, Tan X, Li X and Yao J 2010 *Appl. Phys.* B: *Laser Opt.* **99** 181
[11] Zhong K, Yao J Q, Xu D G, Zhang H Y and Wang P 2011 *Acta Phys. Sin.* **60** 034210 (in Chinese)
[12] Sirtori C, Capasso F, Faist J, Pfeiffer L N and West K W 1994 *Appl. Phys. Lett.* **65** 445
[13] Hiroshima T and Lang R, 1986 *Appl. Phys. Lett.* **49** 456
[14] Dupont E, Wasilewski Z R and Liu H C. 2006 *IEEE J. Electron.* **42** 1157
[15] Cao X L, Wang Y Y, Xu D G, Zhong K, Li J H, Li Z Y, Zhu N N and Yao J Q 2012 *Chin. Phys. Lett.* **29** 014207